

TRIBOELECTRIC NANOGENERATOR BASED ON TRIBOELECTRIFICATION AND MAGNETIC FIELD

Ali A. S.¹, Youssef M. M.², Ali W. Y.³ and Rashed A.³

¹Mechanical Engineering Dept., Faculty of Engineering, Suez Canal University, EGYPT.

²Automotive and Tractors Engineering Dept., Faculty of Engineering, Minia University, P. N. 61111, El-Minia, EGYPT.

³Production Engineering and Mechanical Design Dept., Faculty of Engineering, Minia University, P. N. 61111, El-Minia, EGYPT.

ABSTRACT

The present work discusses the possibility of designing triboelectric nanogenerator (TENG) operated by triboelectrification and magnetic field. The contact-separation and sliding, of polytetrafluoroethylene (PTFE) and polyamide (PA), were operated by the help of magnetic field.

The present work showed that the increase of the intensity of magnetic field caused significant voltage increase. That may be from the ability of magnets to induce magnetic field that was responsible for the voltage increase. Besides, the ESC double layer generated from friction supplies the contacting surfaces by an electric field superimposed on the magnetic field offered by the magnets that is responsible for the increase of the voltage difference. It was observed that inserting steel sheet under PA homogeneously distributed the magnetic field on the contact area. that caused significant voltage increase. Adhering steel wire in form zigzag into the surface of the steel sheet displayed remarkable voltage increase. Further voltage increase was observed for adhering steel wire in spiral form.

KEYWORDS

Triboelectric nanogenerator, magnetic field, polyamide, polytetrafluoroethylene, contact-separation, sliding.

INTRODUCTION

There is growing demand to use renewable and clean energy to reduce the dependency on fossil fuels in order to decrease global warming and climate change, [1 - 3]. TENG can be suitable alternative by harvesting mechanical energy, where contact-separation and sliding on two dissimilar materials can generate ESC, [4, 5]. The TENGs based on contact-separation mode are constructed by adhering two different polarity dielectrics such as nylon (PA) and polytetrafluoroethylene (PTFE) on acrylic board.

The generation of ESC of different intensity and sign on the surface of the dissimilar contacting materials due to the triboelectric effect is carried out using the triboelectric effect, [6 - 8], according to the triboelectric series that may rank materials by acquiring positive or negative charge on the surface of the material. PTFE acquires negative charge after contact-separation with dissimilar material, [9], while PA is located near the top of the triboelectric series and acquires positive charge, [10]. After contact-separation of PTFE and PA, PTFE gains relatively higher value of negative charge, while PA gains relatively higher value of positive charge.

The TENG is made of two dielectric materials that connected to electrodes are on the opposite sides of the triboelectric series. After contact-separation and sliding, the two dielectric surfaces induce equal and opposite ESC on their surface causing potential difference that generates an electric current. The two main applications are energy harvesters, [11 - 14], and self-powered sensor, [15 - 18]. It was revealed that the output open circuit voltage of the TENG could be determined by V-Q-x equation, [19 - 21]. TENGs can be classified into contact-separation type, [22-23] and sliding type, [24 - 25]. Contact-separation type TENG is constructed from two dielectric surfaces separated by an elastic spacer.

The influence of induction on ESC generated on the surface of polymers slid on PA, polypropylene (PP), and PTFE was investigated, [26 - 29], where carbon fibers as well as metallic wires reinforcing PE sliding on PA showed relatively higher values of ESC. Steel wires showed the highest values of ESC due to the generation of an E-field inside the PE matrix.

Recently, it was revealed that providing PTFE surface sliding on PA with insulated copper wires increased the voltage generated due to the electrostatic charge (ESC), [30 - 31]. It was thought that an electric field was generated from the double layer of ESC on the contact surfaces of PTFE and PA generated. In addition to that, the induced electric current by the copper wires generated extra electric field on the sliding surfaces leading to the voltage increase. The induced electric field could be enhanced by wrapping the copper wires on the surface of hollow box of certain height.

In the present work, TENG that can harvest mechanical energy by combining contact-electrification enhanced by magnetic field electrostatic induction was proposed.

EXPERIMENTAL

The test specimens were prepared from wooden cube of $40 \times 40 \times 40 \text{ mm}^3$, covered by aluminium film (Al) of 0.25 mm thickness to work as the first terminal. PTFE film of 0.25 mm thickness was adhered on the Al film representing the first dielectric surface. The tested PA was in form of textile adhered on Al film (second terminal) that covered the wooden block representing the second dielectric surface. The load was applied by weights (0.3 N). The sliding distance was 200 mm. The details of the test specimens are shown in Fig. 1. Permanent magnets of different intensity were

used to apply the magnetic field to investigate the effect of induction on the generated ESC. The magnets were in form of discs of 20 and 60 mG. The experiments were repeated five times to measure the voltage difference. The test procedure contained contact-separation, where the load was applied for five seconds followed by the measurement of the voltage, as well as sliding.

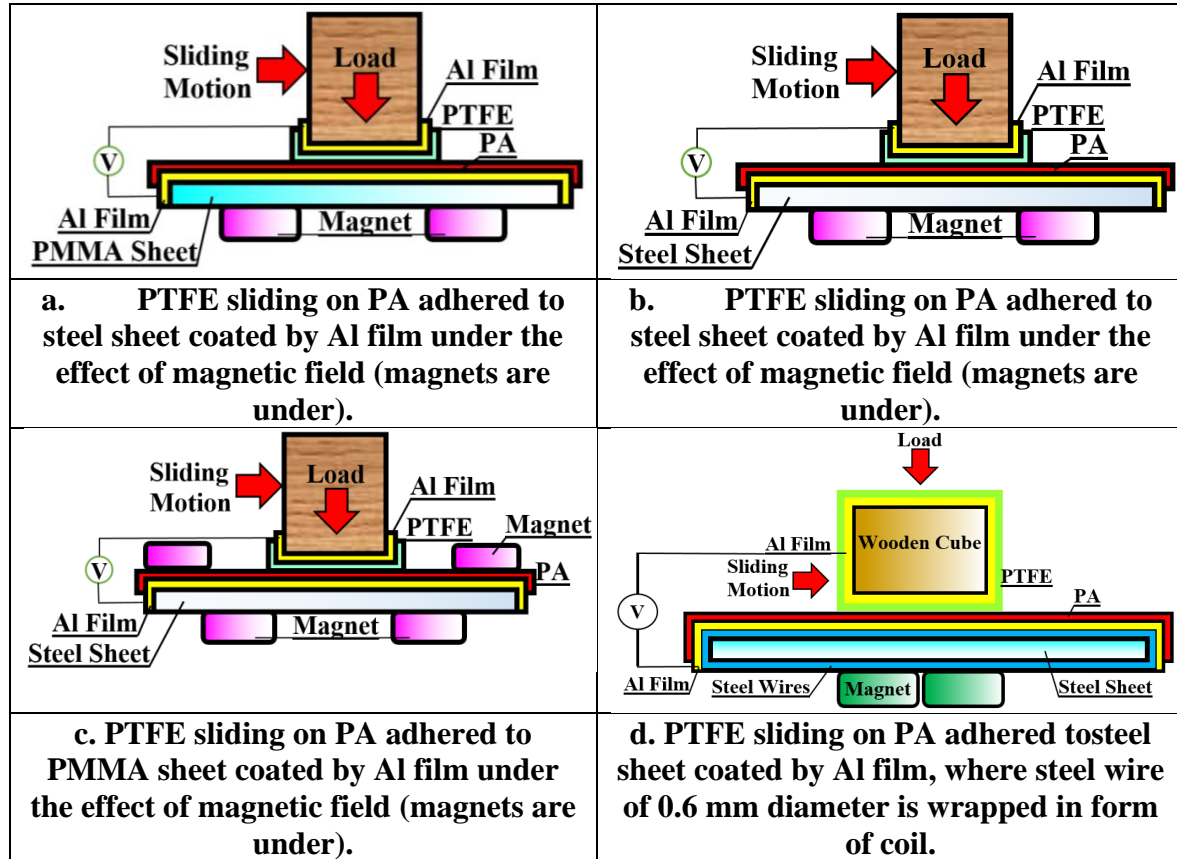


Fig. 1 Details of the test specimens.

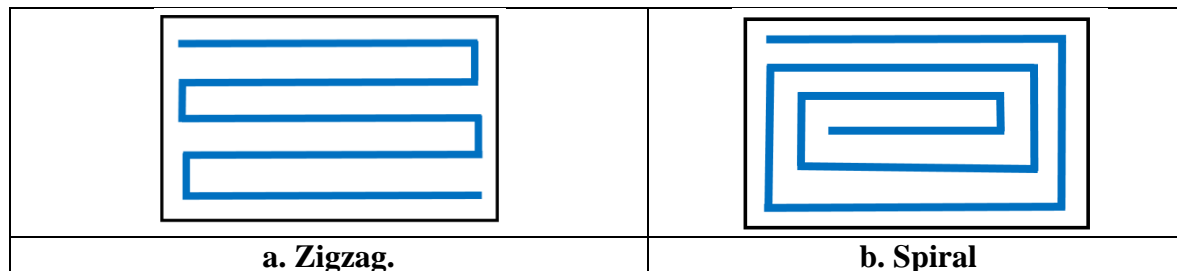


Fig. 2 Form of the steel wire wrapped on the steel sheet, a. Zigzag and b. Spiral.

RESULTS AND DISCUSSION

Triboelectrification is the gain or loss of ESC due to friction, where electron carries the charge transferred from one of the contacting surface to the other during contact-separation and sliding of polymeric materials. Figure 3 shows the voltage

difference generated and measured in mV after contact-separation as well as sliding of PTFE on PA adhered to PMMA sheet, where the permanent magnets were placed under. The details of the test specimens are shown in Fig. 1, a. It is clearly seen that voltage difference displayed by contact-separation was lower than that measured for sliding. Besides, the increase of magnetic fields caused significant voltage increase. This behavior may be related to the double layer of ESC generated on the contact surfaces induced an extra electric field on the sliding surfaces leading to the voltage increase.

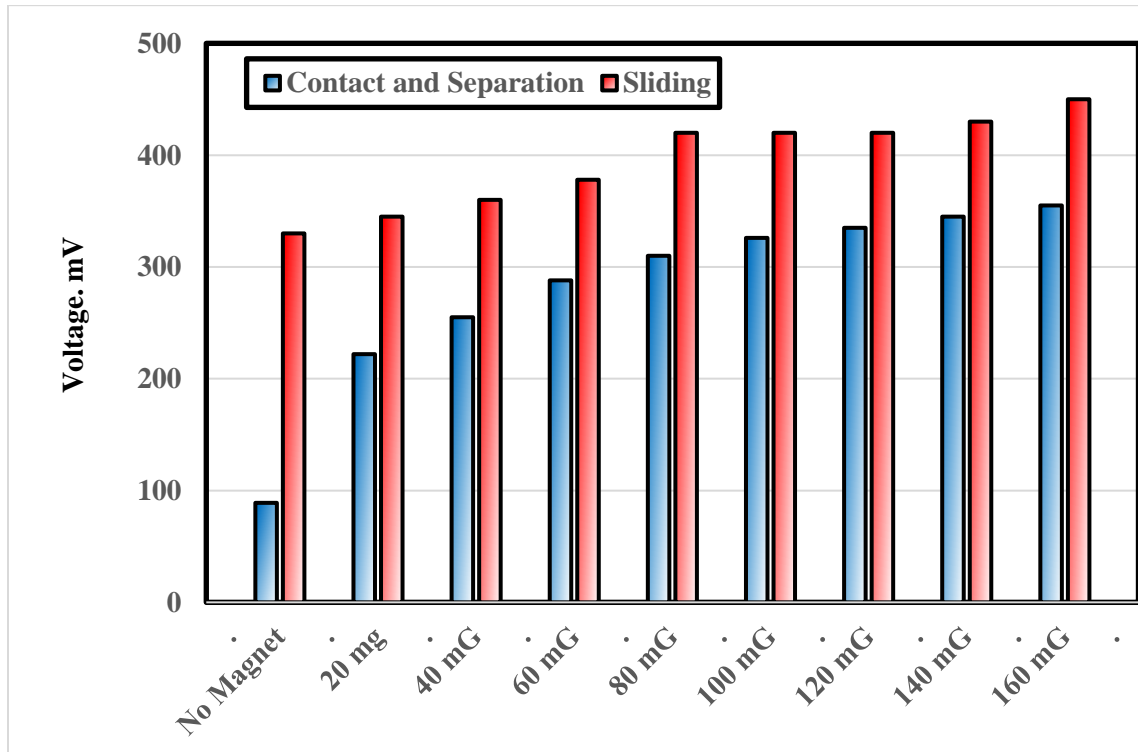


Fig. 3 The voltage difference between PTFE and PA adhered to PMMA sheet.

The increase of voltage difference caused by magnetic field can be explained in terms that the magnets were able to induce magnetic field that was responsible for the voltage increase. Figure 4 illustrates the generation of relatively higher voltage due to the effect of the magnets, where the double layer of ESC generated from friction supplies the system by an electric field superimposed on the magnetic field that is responsible for the increase of the voltage difference.

When the intensity of the magnetic field increased up to 240 mG, the same trend was observed where the highest values of the field were observed at 240 mG, Fig. 5, where voltage difference reached 530 mV after sliding, while that recorded for contact-separation was 410 mV. It seems that the charges during contact were trapped on the two contacted surfaces leading to the increase of voltage difference. Further increase in the intensity of the magnetic field up to 600 mG, Fig. 6, slightly increased the voltage up to 420 and 620 mV after contact-separation and sliding respectively.

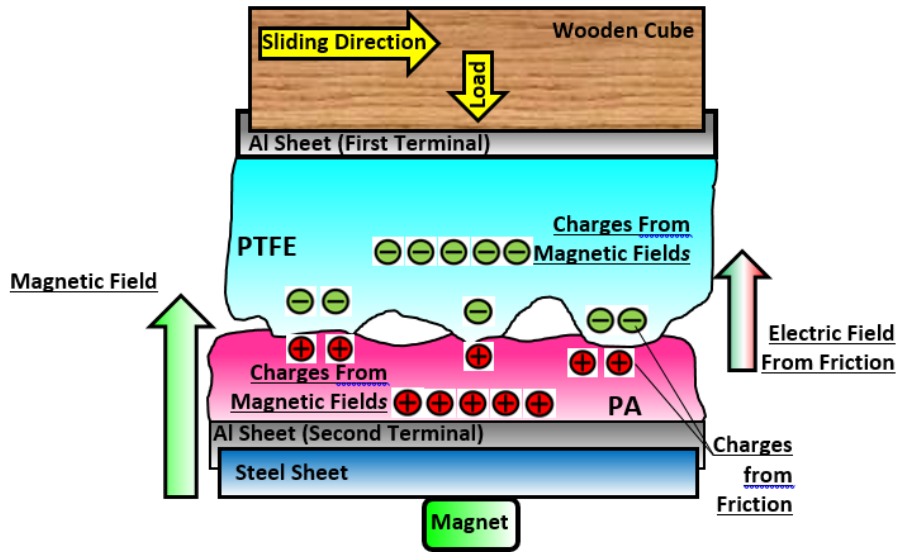


Fig. 4 Explanation of the generation of relatively higher voltage due the effect of the magnetic field.

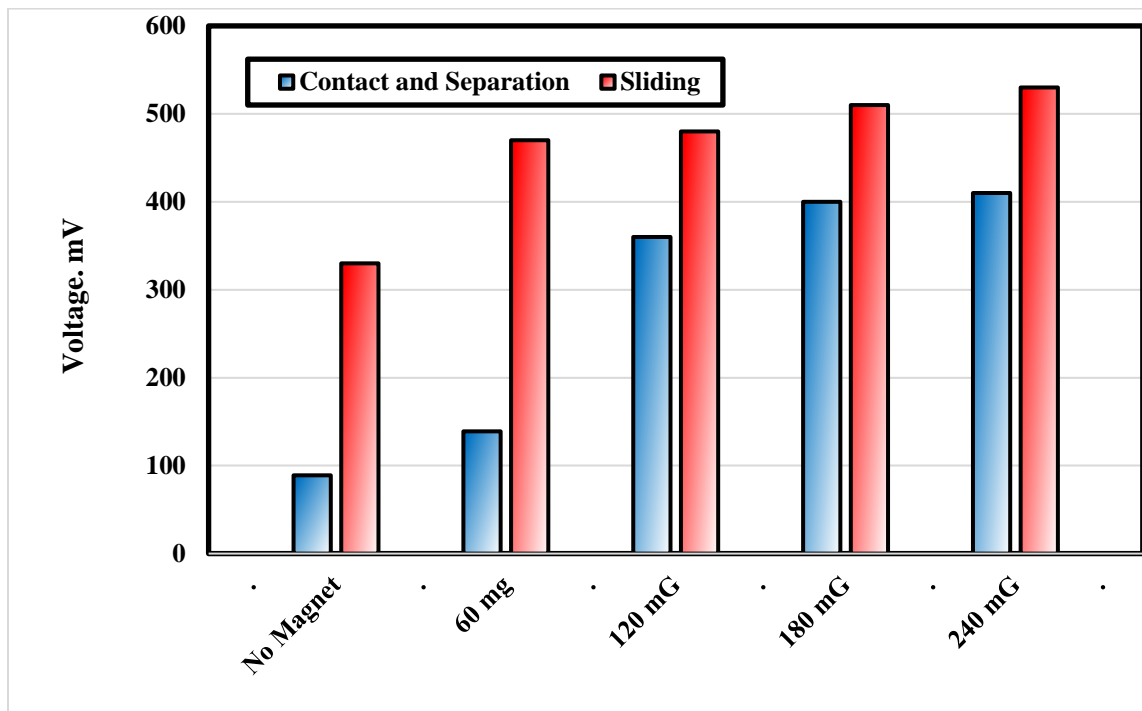


Fig. 5 The voltage difference between PTFE and PA adhered to PMMA sheet for relatively higher values in the magnetic field.

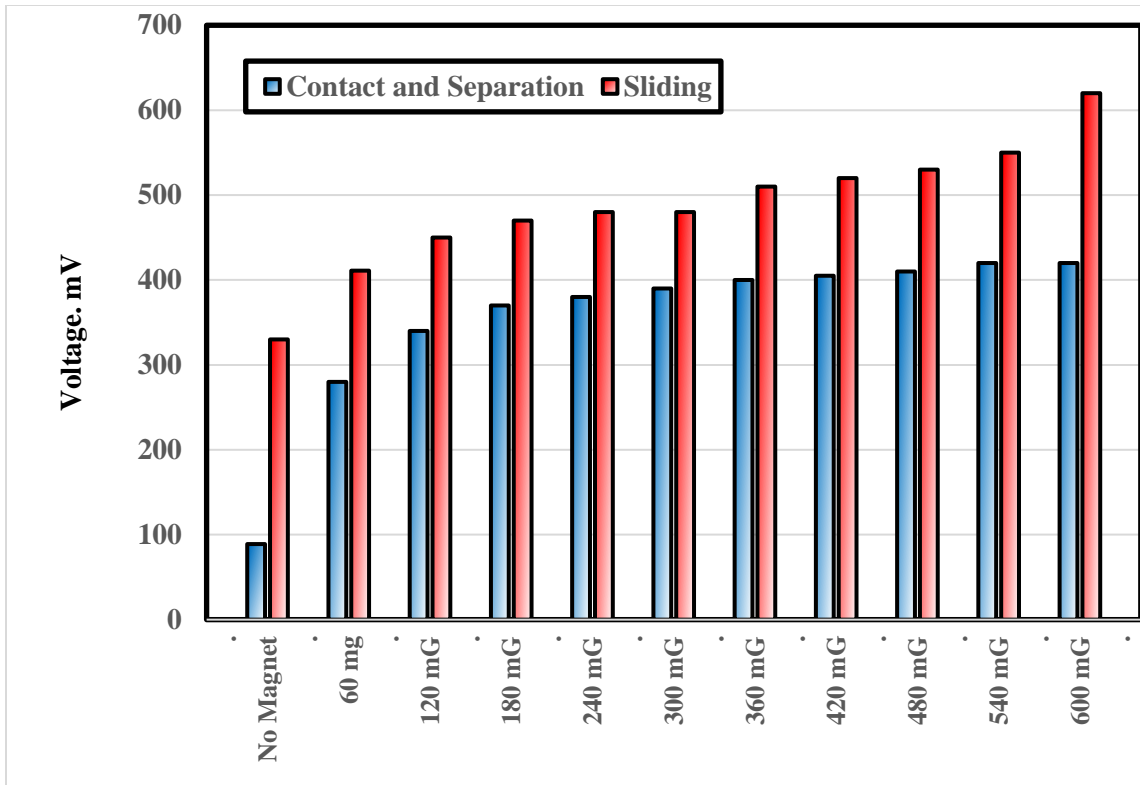


Fig. 6 The voltage difference between PTFE and PA adhered to PMMA sheet for relatively higher values in the magnetic field up to 600 mG.

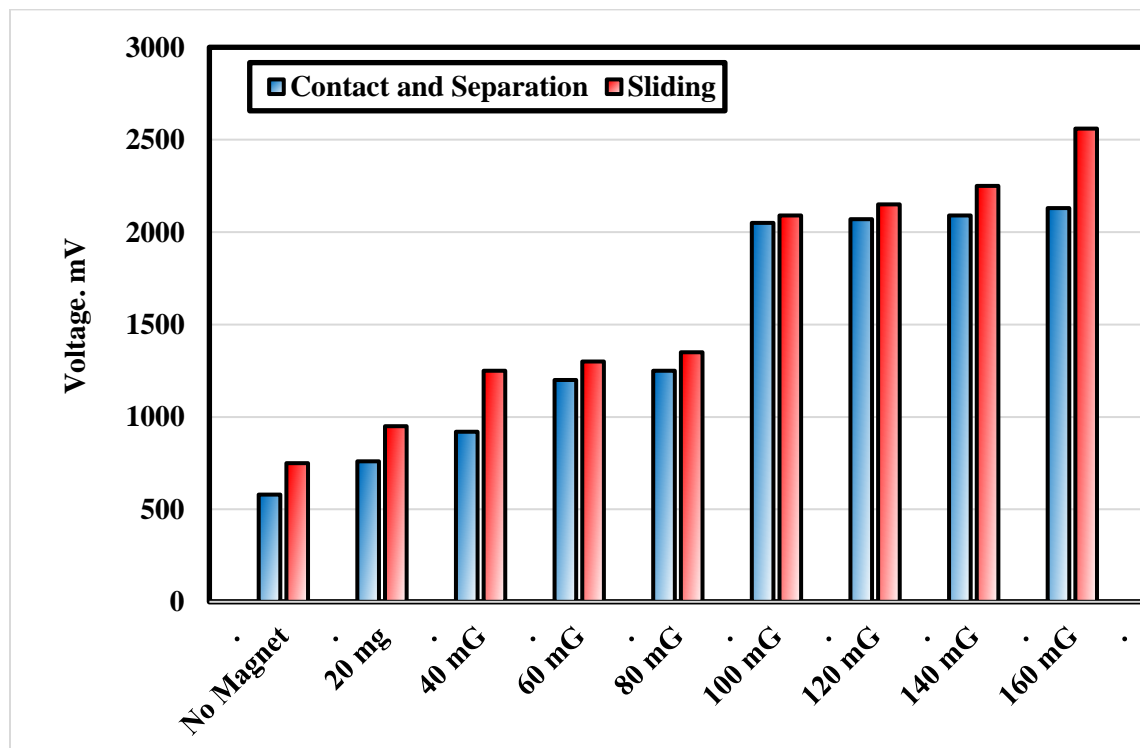


Fig. 7 The voltage difference between PTFE and PA adhered to steel sheet,

(magnets are under).

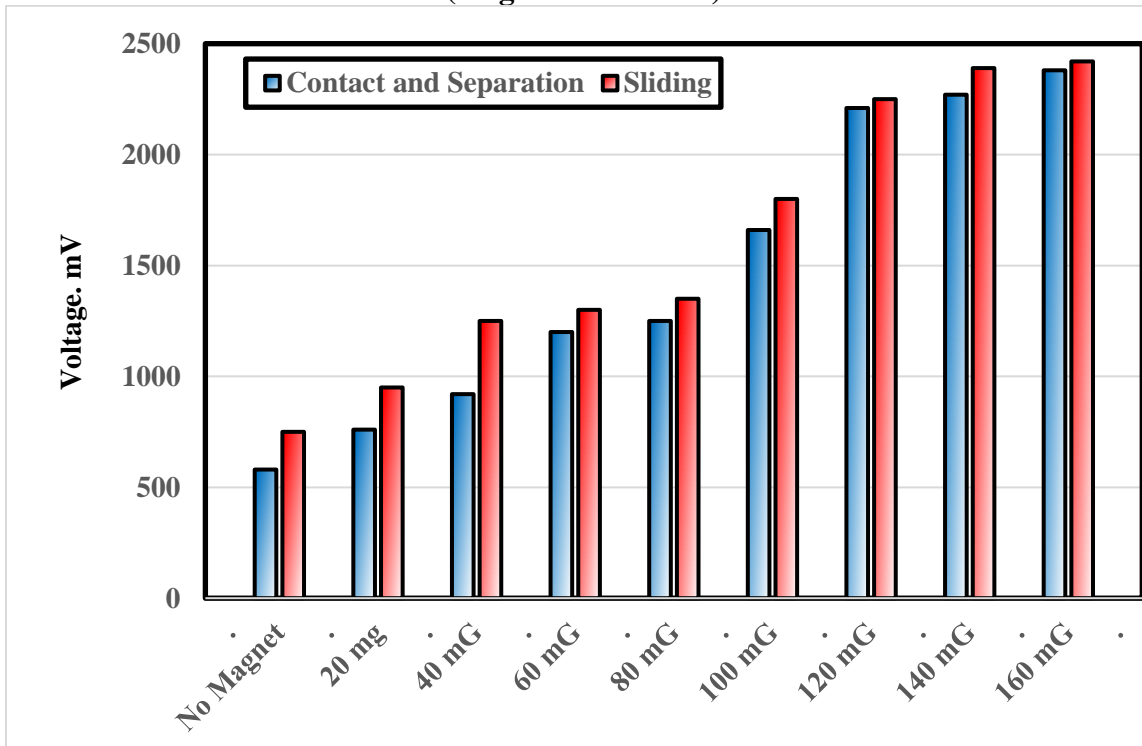


Fig. 8 The voltage difference between PTFE and PA adhered to steel sheet, (magnets are under and above).

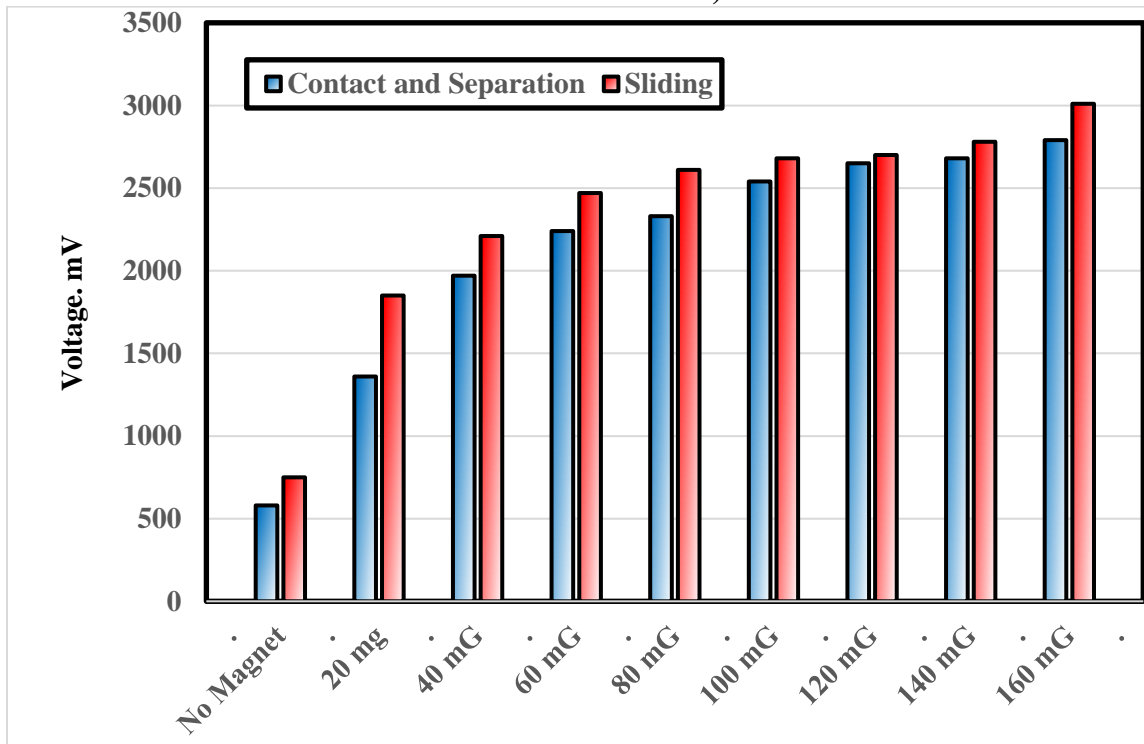


Fig. 9 The voltage difference between PTFE and PA adhered to steel sheet, (magnets are turned over to change their polarity).

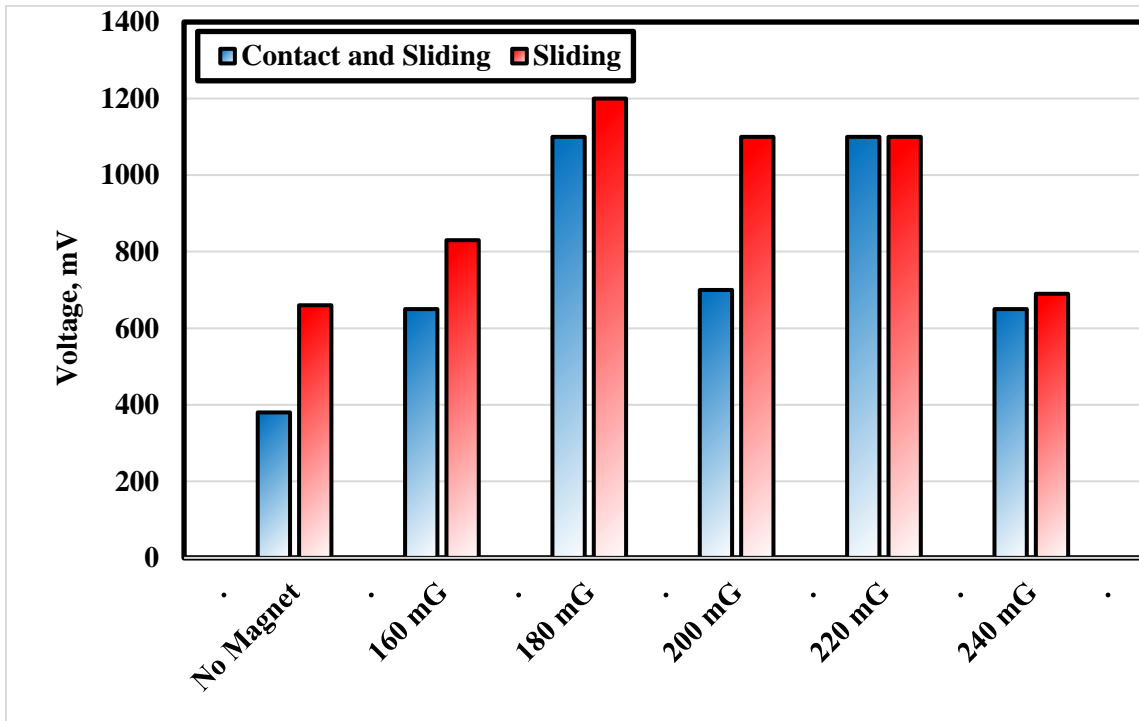


Fig. 10 The voltage difference between PTFE and PA adhered to steel sheet wrapped by steel wire of 0.6 mm diameter in form of coil.

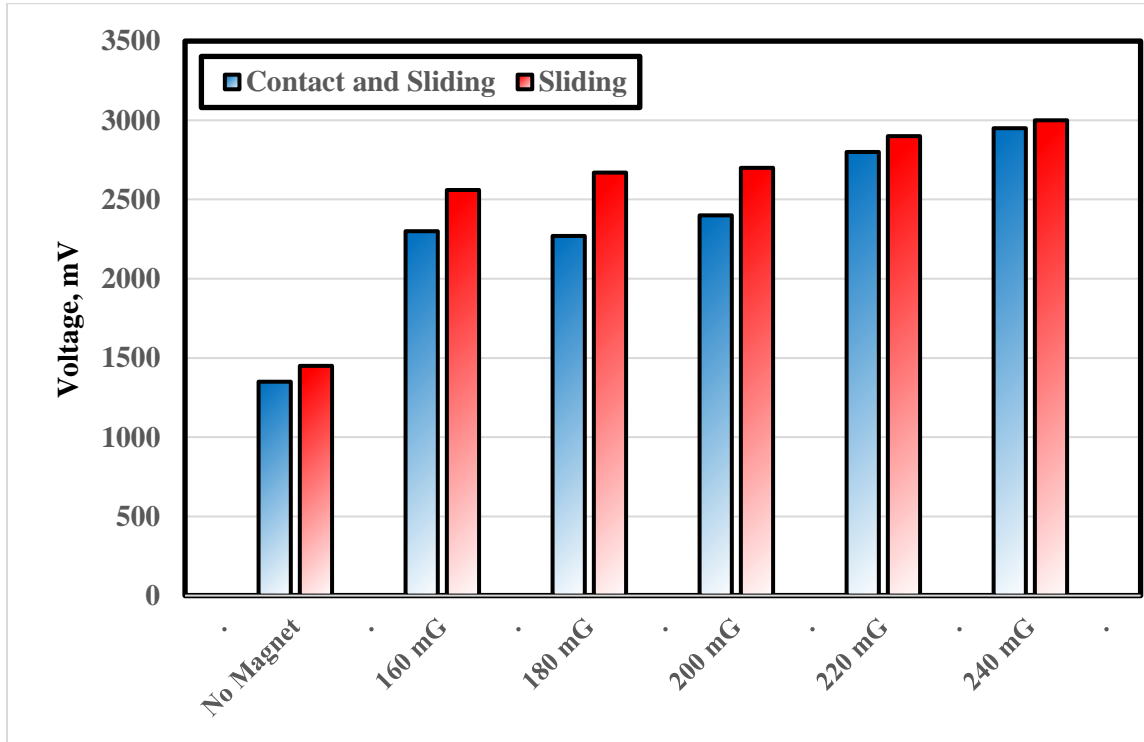


Fig. 11 The voltage difference between PTFE and PA adhered to steel sheet wrapped by steel wire of 0.6 mm diameter in zigzag form.

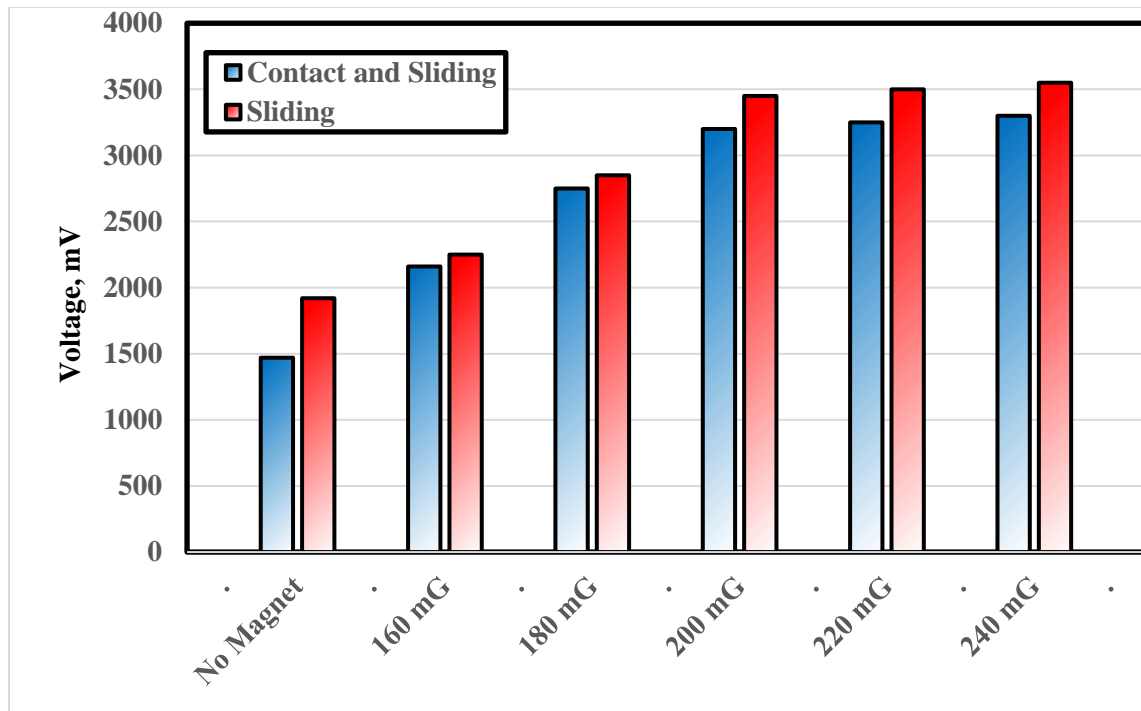


Fig. 12 The voltage difference between PTFE and PA adhered to steel sheet wrapped by steel wire of 0.6 mm diameter in spiral form.

When the PMMA sheet was replaced by steel sheet, Fig. 7, where the magnets were assembled under the steel sheet, Fig. 1, b, the voltage showed remarkable rise with increasing the magnetic field. The voltage difference at 160 mG recorded 2130 and 2560 mV after contact-separation and sliding respectively. It seems the steel sheet homogeneously distributed the magnetic field on the contact area. When the magnets were assembled under and above the PA surface, Figs. 8 and 1, c, slight voltage increase was observed after contact-separation. Figure 9 shows the relationship between voltage and the intensity of the magnetic field when the polarity of the magnets were changed by turning over the magnets. It was observed that voltage recorded relatively higher values up to 2790 and 3010 mV after contact-separation and sliding respectively at 160 mG.

In order to increase the intensity of the magnetic field, the steel sheet was wrapped by steel wire of 0.6 mm diameter in form of coil, Fig. 1, d. The results are shown in Fig. 10, drastic decrease in voltage values was recorded although the value of magnetic field increased up to 240 mG. It seems that magnetic field generated from the steel wire opposed that induced by the permanent magnets. The highest voltage value was 1200 mV at 180 mG after sliding. Changing the form of the steel coil into zigzag, Fig. 2, a, caused significant increase in the voltage values up to 2950 and 3000 mV at 240 mG after contact-separation and sliding respectively, Fig. 11. Further rise, in the voltage values, was detected for the spiral steel wire, Fig. 2, b. Figure 12 shows the voltage difference between PTFE and PA, where the highest values were observed after contact-separation and sliding up to 3300 and 3550 mV at 240 mG.

CONCLUSIONS

1. Voltage difference displayed by contact-separation was lower than that measured for sliding.
2. Increase of magnetic field caused significant voltage increase.
3. Introducing steel sheet increased the magnetic field that caused significant voltage increase.
4. Adhering steel sheet into the surface of the steel sheet displayed remarkable voltage increase.
5. Further voltage increase was observed for adhering steel wire in spiral form.

REFERENCES

1. Gielen D., Boshell F. and Saygin D., "Climate and energy challenges for materials science", *Nat. Mater.* 15 (2), pp. 117 - 120, (2016).
2. Fan F.R., Tian Z.Q. and Wang Z.L., "Flexible triboelectric generator", *Nano Energy* 1 (2), pp. 328 - 334, (2012).
3. Schiermeier Q., Tollefson J., Scully T., Witze A. and Morton O., "Electricity without carbon", *Nature* 454 (7206), pp. 816 - 823, (2008).
4. Lowell J. and Truscott W. S., "Triboelectrification of Identical Insulators: II. Theory and Further Experiments", *J. Phys. D: Appl. Phys.*, 19, pp. 1281-1298, (1986).
5. Baytekin H. T. and Patashinski A. Z., Branicki M., Baytekin B., Soh S. and Grzybowski B. A., "The Mosaic of Surface Charge in Contact Electrification", *Science*, 333, pp. 308 - 312, (2011).
6. Zou H., Zhang Y., Guo L., Wang P., He X., Dai G., Zheng H., Chen C., Wang A. C., Xu C. and Wang Z. L., "Quantifying the triboelectric series", *Nature communications*, Vol. 10, No. 1, pp. 1427, (2019).
7. Diaz A. F., and Felix-Navarro R. M., "A semi-quantitative tribo-electric series for polymeric materials: the influence of chemical structure and properties", *Journal of Electrostatics*, Vol. 62, No. 4, pp. 277-290, (2004).
8. Burgo A. L., Galembeck F., and Pollack G. H., "Where is water in the triboelectric series?", *Journal of Electrostatics* Vol. 80, pp. 30 - 33, (2016).
9. Zhang R. and Olin H., "Material choices for triboelectric nanogenerators: a critical review." *EcoMat*, Vol. 2, No. 4, pp. 120 - 132, (2020).
10. Al-Kabbany A. M., and Ali W. Y., "Reducing the electrostatic charge of polyester by blending by polyamide strings", *Journal of the Egyptian Society of Tribology*, Vol. 16, No. 4, pp. 36 - 44, (2019).
11. Yang Y., Zhu G., Zhang H., Chen J., Zhong X., Lin Z. H., Su Y., Bai P., Wen X. and Wang Z. L., "Triboelectric nanogenerator for harvesting wind energy and as self-powered wind vector sensor system.", *ACS nano*, Vol. 7, No. 10, pp. 9461 - 9468, (2013).
12. Zhang H., Yang Y., Su Y., Chen J., Adams K., Lee S., Hu C. and Wang, Z. L., "Triboelectric nanogenerator for harvesting vibration energy in full space and as self powered acceleration sensor", *Advanced Functional Materials*, Vol. 24, No. 10, pp. 1401 - 1407, (2014).
13. Cheng P., Guo H., Wen Z., Zhang C., Yin X., Li X., Liu D., Song W., Sun X., Wang J. and Wang Z. L., "Largely enhanced triboelectric nanogenerator for

efficient harvesting of water wave energy by soft contacted structure.", *Nano Energy*, Vol. 57, pp. 432 - 439, (2019).

14. Wang X., Niu S., Yin Y., Yi F., You Z. and Wang Z. L., "Trieoelectric nanogenerator based on fully enclosed rolling spherical structure for harvesting low-frequency water wave energy", *Advanced Energy Materials*, Vol. 5, No. 24, 1501467, (2015).

15. Jin T., Sun Z., Li L., Zhang Q., Zhu M., Zhang Z., Yuan G., Chen T., Tian Y., Hou X. and Lee C., "Trieoelectric nanogenerator sensors for soft robotics aiming at digital twin applications", *Nature communications*, Vol. 11, No .1, pp, 1 - 12, (2020).

16. Qin K., Chen C., Pu X., Tang Q., He W., Liu Y., Zeng Q., Liu G., Guo H. and Hu C., "Magnetic array assisted trieoelectric nanogenerator sensor for real-time gesture interaction.", *Nano-micro letters*, Vol. 13, No. 1, pp. 1-9, (2021).

17. Zhou Q., Pan J., Deng S., Xia F. and Kim T., "Trieoelectric Nanogenerator Based Sensor Systems for Chemical or Biological Detection", *Advanced Materials*, Vol. 33, No. 35, 2008276, (2021).

18. Dhakar L., Pitchappa P., Tay F. E. H. and Lee C., "An intelligent skin based self-powered finger motion sensor integrated with trieoelectric nanogenerator", *Nano Energy*, Vol. 19, pp, 532-540, (2016).

19. Niu S., Wang S., Lin L., Liu Y., Zhou Y. S., Hu Y. and Wang Z. L., "Theoretical study of contact-mode trieoelectric nanogenerators as an effective power source", *Energy & Environmental Science*, Vol. 6, No. 12, pp. 3576-3583, (2013).

20. Dharmasena R. D. I. G., Jayawardena K. D. G. I., Mills C.A., Dorey R. A. and Silva S. R. P., "A unified theoretical model for Trieoelectric Nanogenerators", *Nano Energy*, Vol. 48, pp. 391-400, (2018).

21. Xu Y., Min G., Gadegaard N., Dahiya R. and Mulvihill D. M., "A unified contact force-dependent model for trieoelectric nanogenerators accounting for surface roughness", *Nano Energy*, Vol. 76, 105067, (2020).

22. Zhu G., Lin Z. H., Jing Q., Bai P., Pan C., Yang Y., Zhou Y. and Wang Z. L., "Toward large-scale energy harvesting by a nanoparticle-enhanced trieoelectric nanogenerator.", *Nano letters*, Vol. 13, No. 2, pp. 847 - 853, (2013).

23. Chen J., Zhu G., Yang W., Jing Q., Bai P., Yang Y., Hou T. C. and Wang Z. L., "Harmonic-resonator-based trieoelectric nanogenerator as a sustainable power source and a self-powered active vibration sensor" *Advanced materials*, Vol. 25, No. 42, pp. 6094 - 6099, (2013).

24. Wang S., Lin L., Xie Y., Jing Q., Niu S. and Wang Z. L., "Sliding-trieoelectric nanogenerators based on in-plane charge-separation mechanism", *Nano letters*, Vol. 13, No. 5, pp. 2226 - 2233, (2013).

25. Lin L., Wang S., Xie Y., Jing Q., Niu S., Hu Y. and Wang Z. L., "Segmentally structured disk trieoelectric nanogenerator for harvesting rotational mechanical energy", *Nano letters*, Vol. 13, No. 6, pp. 2916 - 2923, (2013).

26. Ali A. S., Khashaba M. I., "Effect of Copper Wires Reinforcing Polyethylene on Generating Electrostatic Charge", *EGTRIB*, Vol. 13, No. 4, October 2016, pp. 28 - 40, (2016).

27. Ali A. S., Youssef Y. M., Khashaba M. I. and Ali W. Y., "Electrostatic Charge Generated From Sliding of Polyethylene Against Polytetrafluoroethylene", *EGTRIB Journal*, Vol. 14, No. 3, July 2017, pp. 34 – 49, (2017).

28. Ali A. S., Youssef Y. M., Khashaba M. I. and Ali W. Y., “Dependency of Friction on Electrostatic Charge Generated on Polymeric Surfaces”, EGTRIB Journal, Vol. 14, No. 3, July 2017, pp. 50 – 65, (2017).
29. Alahmadi A., Ali A. S. and Ali W. Y., "Electrostatic Charge Generated from Sliding of High Density Polyethylene Against Air Bubble Sheet of Low Density Polyethylene", EGTRIB Journal, Vol. 14, No. 4, October 2017, pp. 27 – 39, (2017).
30. Ali A. S., Youssef M. M., Ali W. Y. and Elzayady N., “Triboelectric Nanogenerator Based on Contact and Separation as well as Sliding of Polyamide on Polytetrafluoroethelene”, Journal of the Egyptian Society of Tribology, Vol. 20, No. 1, January 2023, pp. 32 – 40, (2023).
31. Ali A. S., Youssef M. M., Ali W. Y. and Rashed A., “Enhancing the Efficiency of Triboelectric Nanogeneratorby Electrostatic Induction”, Journal of the Egyptian Society of Tribology, Vol. 20, No. 1, January 2023, pp. 41 – 50, (2023).